ELSEVIER

Advan. Enzyme Regul. 44 (2004) 37–49

ADVANCES IN ENZYME REGULATION

www.elsevier.com/locate/advenzreg

Sequence variants in the 3′→5′ deoxyribonuclease TREX2: identification in a genetic screen and effects on catalysis by the recombinant proteins

Fred W. Perrino[a,*], Anna Krol[a], Scott Harvey[a], S. Lilly Zheng[b], David A. Horita[a], Thomas Hollis[a], Deborah A. Meyers[b], William B. Isaacs[c], Jianfeng Xu[b]

[a] *Department of Biochemistry, Wake Forest University Health Sciences, Winston-Salem, NC 27157, USA*
[b] *Center for Human Genomics, Wake Forest University Health Sciences, Winston-Salem, NC 27157, USA*
[c] *Brady Urological Institute Research Laboratories, Johns Hopkins School of Medicine, Baltimore, MD 21287, USA*

Introduction

The excision of nucleotides from DNA 3′ termini is an important step in DNA replication, repair, and recombination pathways to generate the correctly base paired termini needed for subsequent processing. The 3′→5′ deoxyribonucleases are the enzymes that catalyze the 3′ excision of nucleoside monophosphates from DNA to provide this cellular function. Since the seminal work of Lindahl (1969) there have been several reports in the literature of 3′→5′ deoxyribonuclease activities identified from a variety of eukaryotic cell types (Hollis and Grossman, 1981; Mosbaugh and Meyer, 1980; Skalski et al., 1995; Skarnes et al., 1986; Bialek and Grosse, 1993; Brown et al., 2002), including an exonuclease activity purified in the Perrino laboratory from human and bovine cells (Perrino et al., 1994, 1999). Sequencing of peptides generated from the purified bovine (Mazur and Perrino, 1999) and rabbit (Hoss et al., 1999) proteins containing this 3′→5 deoxyribonuclease activity resulted in the discovery of the two closely related genes named TREX1 and TREX2 (Mazur and Perrino, 1999, 2001a, b; Hoss et al., 1999). In addition to the TREX genes other mammalian genes have been reported to encode proteins containing 3′→5′ exonuclease activities. These genes include the human apurinic/apyrimidinic endonuclease APEX (Wilson et al., 1995; Chaudhry et al., 1999; Chou et al., 2000), Werner syndrome (*WRN*) (Shen et al., 1998; Kamath-Loeb et al., 1998; Huang et al., 1998), *p53* (Mummenbrauer et al., 1996), *hRAD1* (*Ustilago maydis*

*Corresponding author.

0065-2571/$ - see front matter
doi:10.1016/j.advenzreg.2003.11.010

REC1) (Parker et al., 1998; Thelen et al., 1994), *hRAD9* (Bessho and Sancar, 2000), and *hMRE11* (Paull and Gellert, 1998, 2000). The genes that encode these 3′ nucleotide excising enzymes indicate an apparently diverse collection of proteins that likely reflect the multiple pathways present in human cells for the modification of DNA 3′ termini during DNA metabolism. Genetic defects have not yet been identified in the TREX genes, but defects in other exonuclease genes indicate functions in various pathways of DNA replication, repair, and recombination.

The genes encoding the TREX1 and TREX2 $3' \rightarrow 5'$ deoxyribonucleases are located on chromosomes 3p21.2–21.3 and Xq28, respectively. The 314-amino-acid TREX1 and the 236-amino-acid TREX2 proteins are encoded in single open reading frames with potential transcriptional start sites located −140 and −650 base pairs upstream of TREX1 and −623 and −753 base pairs upstream of TREX2 (Mazur and Perrino, 2001b). Transcription of the TREX genes has been detected in all human tissues that have been tested indicating a possible housekeeping function for these enzymes, such as might be required in the DNA repair processes necessary to maintain the integrity of the human genome. Further, the biochemical properties of the TREX $3' \rightarrow 5'$ deoxyribonucleases suggest that these enzymes contribute in human cells to the maintenance of genetic integrity by removing mispaired 3′ nucleotides to generate correctly paired 3′ termini that are required for efficient processing by DNA enzymes such as the DNA polymerases or ligases (Mazur and Perrino, 2001a).

Several possible roles for the TREX $3' \rightarrow 5'$ deoxyribonucleases in human cells must be considered. Replication and repair of the 2.9 billion base pair human genome is a multi-step process that includes hundreds of enzymes and is orchestrated largely from the 3′ terminus of the deoxyribonucleotide chain. A non-Watson–Crick base pair in DNA positioned at the 3′ terminus creates a DNA end that is kinetically unfavorable to further polymerization: essentially a kinetic block that requires excision by a $3' \rightarrow 5'$ deoxyribonuclease. There are at least 14 DNA polymerases functioning in human cells (Burgers et al., 2001); only three contain inherent 3′ exonuclease activities. It is possible that TREX1 or TREX2 excise nucleotides misincorporated by one or more of these DNA polymerases, thus acting as proofreading enzymes to alleviate the kinetic block to elongation. To consider this possibility one must expand the currently accepted view of proofreading that has been mostly limited to the removal of misinserted nucleotides by the DNA polymerase-associated exonucleases. As an alternative mechanism for proofreading one of the TREX enzymes might be directed to a kinetically blocked 3′ terminus resulting from a 3′-terminal mismatch. This proofreading mechanism would have relevance also to the presence of a damaged base pair or a nucleotide analog that creates a kinetic block at the 3′ terminus. Anti-cancer and anti-viral therapeutic strategies that target DNA metabolism frequently include nucleotide analogs that block polymerization upon incorporation at the 3′ terminus of a growing DNA chain. Proofreading by the TREX proteins of these nucleotide analogs would result in the excision of these analogs and limit their efficacy. Our current understanding of the mismatch repair process in human cells indicates that a $3' \rightarrow 5'$ deoxyribonuclease

is required when the strand break is positioned 3′ to the mismatch (Modrich, 1997). The TREX proteins could provide this necessary activity during DNA mismatch repair in human cells. The DNA recombination pathways involved in double-strand break repair indicate the requirement for a $3' \rightarrow 5'$ deoxyribonuclease that might be provided by a TREX protein to remove unpaired 3′ ends permitting the following ligation step. The robust catalytic efficiencies of the TREX enzymes make these proteins well suited for 3′ nucleotide excision in many of the DNA repair pathways where remodeling of the 3′ end is necessary.

Genetic and biochemical studies of the TREX genes and proteins will be required to elucidate cellular function. There were two objectives of the work presented in this paper: (1) to identify single nucleotide polymorphisms (SNPs) in the TREX2 gene that might relate to genetic susceptibilities in human prostate cancer and (2) to establish an improved protein expression system to generate the TREX2 variant proteins for biochemical studies. A genomewide search for hereditary prostate cancer (HPC) susceptibility genes indicated the presence of a HPC locus on the X chromosome at Xq27–28 (Smith et al., 1996). A combined fine mapping linkage analysis in 360 HPC families confirmed this linkage and defined location of the most likely HPC locus to a $\sim$20 cM region, flanked by the markers DXS984 and DXS1108 (Xu et al., 1998). Based on the database of UCSC Genome Bioinformatics, this linkage region locates at 138–153 Mb on X chromosome. The TREX2 gene, which locates at 151 Mb, is within the telomeric side of this most likely linkage region. Our genetic analysis of TREX2 identified three missense SNPs resulting in the S39F, R137C, and R156L TREX2 variant proteins. These three TREX2 variant proteins and the wild-type TREX2 were prepared using a novel intein-based protein expression system, and the kinetic parameters that govern 3′ nucleotide excision by these four TREX2 proteins were determined.

Materials and methods

The genetic screen for TREX2 variants. The study subjects were ascertained at the Brady Urology Institute at Johns Hopkins Hospital (Baltimore, MD). The eligibility criterion for HPC was at least three first-degree relatives affected with prostate cancer. The diagnosis of prostate cancer was verified by medical records for each affected male studied. All individuals that participated in this study gave full informed consent. The PCR products of the 1.7 kb genomic sequence that includes the entire TREX2 open reading frame and part of the promoter were directly sequenced. The primers for the PCR are available upon request. All PCR reactions were performed in a 10 μl volume consisting of 30 ng of genomic DNA, 0.2 μM of each primer, 0.2 mM of each dNTP, 1.5 mM $MgCl_2$, 20 mM Tris-HCl, 50 mM KCl, and 0.5 U Taq polymerase (Life Technologies, Inc.). PCR cycling conditions were as follows: 94°C for 4 min; followed by 30 cycles of 94°C for 30 s, specified annealing temperature for 30 s, and 72°C for 30 s; with a final extension of 72°C for 6 min. All PCR products were purified using the QuickStep™ PCR purification Kit (Edge BioSystems, Gaithersburg, MD) to remove dNTPs and excess primers. All

sequencing reactions were performed using dye-terminator chemistry (BigDye, ABI, Foster City, CA) and then precipitated using $63 \pm 5\%$ ethanol. Samples were loaded onto an ABI 3700 DNA Analyzer after dissolving in 20 μl H_2O. SNPs were identified using Sequencher™ software version 4.0.5 (Gene Codes Corporation).

Construction of plasmids encoding self-cleaving TREX2 fusion proteins. The bacterial plasmid pMYCT2(AG) was engineered to encode a single fusion protein composed of the maltose binding protein (MBP), the *Saccharomyces cerevisiae* vacuolar membrane ATPase intein (Intein) with the chitin binding domain (CBD), and the human TREX2 protein (Fig. 2). To prepare this vector an oligonucleotide linker containing the *Sac*II/*Not*I/*Sal*I/*Pst*I restriction sites was cloned into a *Sac*II/*Pst*I digested pMYB5 plasmid (New England Biolabs, Beverly, MA) to generate the plasmid pMY. The Intein containing the CBD (Chong et al., 1998) was recovered using polymerase chain reaction (PCR) with the pMYB11 plasmid (New England Biolabs, Beverly, MA) as template and with primers that introduced the restriction sites *Bam*HI into the 5′ side and *Xba*I into the 3′ side of the product and eliminated the unique *Bam*HI at the 3′ end of the Intein sequence. The Intein PCR product was digested with *Bam*HI/*Xba*I and cloned into the *Bam*HI/*Xba*I-digested pMAL-TREX2 plasmid (Mazur and Perrino, 2001a) to generate plasmid pMALIntTREX2. A PCR site-directed mutagenesis strategy (Higuchi, 1990) was used to delete DNA sequence encoding unwanted amino–acids at the TREX2 *N*-terminus, and a 5′-GCCGGC-3′ sequence encoding Ala–Gly was added at the TREX2 *N*-terminus generating the pMALIntTREX2(AG) plasmid. The *Kpn*I–*Sal*I fragment was recovered from the pMALIntTREX2(AG) plasmid and cloned into the *Kpn*I–*Sal*I-digested pMY plasmid to generate pMYCT2(AG). Expression from the pMYC-T2(AG) vector generates transcripts encoding the fusion protein MBP-Intein(CBD)-TREX2. The three TREX2 SNPs resulting in amino-acid sequence variants—S39F, R137C, and R156L—were produced using a PCR site-directed mutagenesis strategy (Higuchi, 1990) to generate the TREX2 SNP plasmids pMYCT2(AG)S39F, pMYCT2(AG)R137C, and pMYCT2(AG)R156L.

Overexpression and purification of the recombinant TREX2 proteins. For over-expression of the MBP-Intein(CBD)-TREX2 fusion proteins the pMYCT2(AG) plasmid (or a TREX2 SNP plasmid) was electroporated into *E. coli* BL21(DE3) Rosetta cells (Novagen). Cells were grown in a rich LB medium at 37°C to an $A_{600} = 0.5$, and isopropyl-1-thio-β-D-galactopyranoside was added to a final concentration of 0.5 mM for 10 min. Cell cultures were transferred to shaking water baths at 15°C for an additional 20 h. Cell extracts were prepared by sonication in 20 mM Tris-HCl (pH 7.5), 1 mM EDTA, 200 mM NaCl containing a complete protease inhibitor cocktail (Roche: Cat. no. 1697498). The MBP-Intein(CBD)-TREX2 fusion protein was affinity-purified using an amylose resin (New England Biolabs, Beverly, MA) as described by the manufacturer. Thiol-induced cleavage of the fusion protein was initiated upon addition of dithiothreitol to 40 mM and continued overnight at 25°C. The cleavage reaction was passed over a chitin resin (New England Biolabs, Beverly, MA), and the flow-through fractions were pooled and dialyzed against 50 mM Tris-HCl (pH 7.5), 1 mM EDTA, and 10% glycerol. The sample was loaded onto a phosphocellulose column, washed with the

equilibration buffer, and developed with a 250-ml linear gradient of 0–600 mM NaCl in the equilibration buffer. The peak fractions containing TREX2 were pooled, concentrated to approximately 0.5 mg/ml, and stored in aliquots at −80°C. The TREX2 concentrations were determined by A_{280} using the molar extinction coefficient $\varepsilon = 16{,}860\ M^{-1}\,cm^{-1}$ (Gill and von Hippel, 1989).

Exonuclease assays. The standard exonuclease reactions (10 μl) contained 20 mM Tris-HCl (pH 7.5), 5 mM $MgCl_2$, 2 mM dithiothreitol, 100 μg/ml BSA, 50 nM 5′-^{32}P-labeled dT_{20} oligonucleotide, and TREX2 proteins as indicated in the figure and table legends. Incubations were at 25°C for 20 min. All enzyme dilutions were performed at 0°C in 100 μg/ml BSA. For the kinetic analysis to determine K_M and k_{cat} values the 5′-^{32}P-labeled dT_{20} oligonucleotide concentrations were varied between 5 and 500 nM and TREX2 proteins (10 pg) were used. Reactions were quenched by addition of 30 μl of cold ethanol and dried in vacuo. Pellets were resuspended in 5 μl of formamide, heated to 95°C for 5 min, and separated on 23% denaturing polyacrylamide gels. Radiolabeled bands were visualized and quantified using a Storm phosphorimager (Molecular Dynamics). The amount of dTMP excised in a reaction was determined by calculating the fraction of the total radiolabeled oligomer that was present at each band position within a lane. The fraction of oligomer at each position was multiplied by the number of dTMPs excised from the dT_{20} to generate the oligomer and by the total fmol of dT_{20} in the starting reaction. The sum of these values yielded the total fmol of dTMP excised. The average activities and apparent K_M and k_{cat} values and standard errors for TREX2 and the variant proteins were determined by nonlinear regression using SigmaPlot 8.02 (SPSS Science, Inc.).

Results and discussion

Identification of single nucleotide polymorphisms in the TREX2 gene

A genetic screen of the TREX2 gene was performed in prostate cancer samples to identify mutations and other single nucleotide polymorphisms and to investigate a potential association between TREX2 and prostate cancer susceptibility. Genetic screening of TREX2 in ninety-six prostate cancer samples identified 11 SNPs within the 1.7 kb TREX2 transcript (Fig. 1). Three SNPs result in the S39F, R137C, and R156L amino-acid substitution variants. A genotypic analysis of these SNP variants was performed in a larger sample including a total of 245 sporadic prostate cancer cases and 222 unaffected controls ascertained at the Johns Hopkins Hospital. This genetic analysis shows that all three SNPs are present at low frequencies (approx. 1%). The S39F and R137C SNPs were detected once each in case samples and were not detected in controls. The R156L SNP was detected in four cases and was detected twice in controls. Thus, these genetic data identified three single amino-acid sequence variants of TREX2 that occurred at a frequency too low to permit statistical evaluation in the tested population.

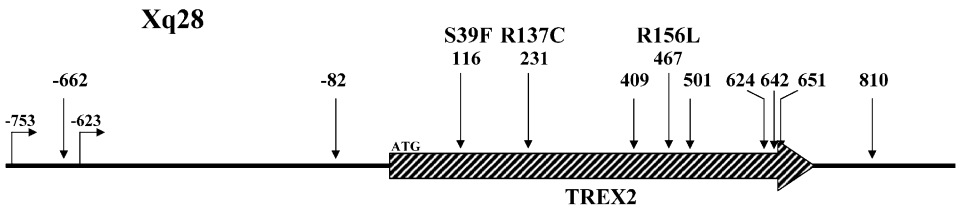

Genotype analysis of the three missense changes using sporadic prostate cancer and unaffected controls

	Case (total=249)	Controls (total=222)
S39F	**1**	**0**
R137C	**1**	**0**
R156L	**4**	**2**

Fig. 1. Single nucleotide polymorphisms (SNPs) in the TREX2 gene identified in prostate cancer samples. The single open reading frame encoding TREX2 on Xq28 and the positions of the identified SNPs are shown. The potential transcriptional start sites at −753 and −623 are indicated. The A of the initiating ATG is nucleotide ♯1.

Preparation of TREX2 and the TREX2-S39F, -R137C, and -R156L proteins

A new bacterial protein expression system was developed that provides high protein expression and convenient affinity purification for the TREX2 proteins. We previously demonstrated high level expression of the TREX2 gene in *E. coli* by preparing a fusion protein construct in which the maltose binding protein was expressed at the *N*-terminus of the TREX2 protein (Mazur and Perrino, 2001a). The 236-amino-acid TREX2 protein was successfully cleaved from the MBPTREX2 fusion protein with Genenase and purified to yield homogenous protein. We have now replaced the protease cleavage sequence with the *Sce* VMA intein sequence in a novel plasmid construct leading to the successful generation of TREX2 and eliminating the need for protease addition to liberate the TREX2 enzyme. To accomplish this it was necessary to engineer a large fusion protein construct in which MBP was positioned at the N-terminus, the *Sce* VMA intein in the center, and TREX2 at the C-terminus (Fig. 2). Overexpression of the MBP-Intein-TREX2 fusion was performed in an *E. coli* cell that also expresses the rare tRNAs to facilitate efficient translation of the human TREX2 gene that contains codons rarely used in *E. coli*. Efficient translation of the MBP and Intein components in this transcript facilitates continued synthesis through the TREX2 protein segment in this fusion construct upon induction of the plasmid in *E. coli* generating 50–100 mg of fusion protein per liter of bacterial culture (Fig. 3, lane 3). The MBP-Intein(CBD)-TREX2 fusion protein was affinity purified using an amylose resin (Fig. 3, lane 4). The *Sce* VMA intein is a self-cleaving protein engineered to direct cleavage at the *N*- and

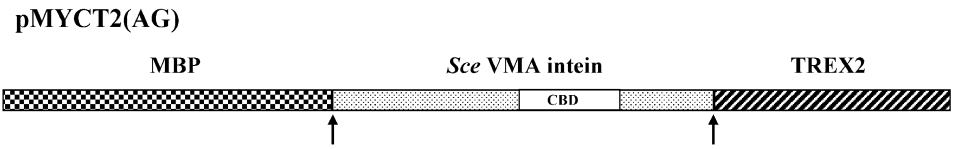

Fig. 2. The TREX2 fusion protein construct. A bacterial plasmid pMYCT2(AG) was engineered to produce a single fusion protein containing the maltose binding protein (MBP), the *Saccharomyces cerevisiae* vacuolar membrane ATPase intein (Intein) with the chitin binding domain (CBD), and the human TREX2 protein. The positions of cleavage upon dithiothreitol addition to the purified fusion protein are indicated by arrows.

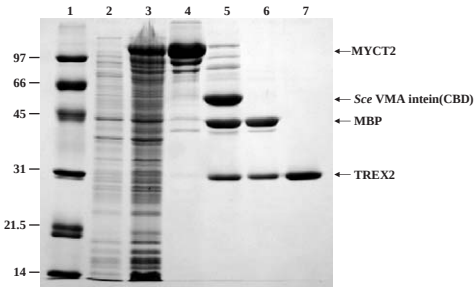

Fig. 3. Purification of TREX2 using the fusion protein construct. A sample of bacterial culture was removed (lane 2) prior to addition of isopropyl-1-thio-β-D-galactopyranoside to induce expression of the MBP-Intein-TREX2 plasmid (lane 3). The fusion protein was affinity-purified from a cell extract using an amylose resin (lane 4). Dithiothreitol to 40 mM was added, and the sample was incubated overnight at 25°C (lane 5). The cleaved proteins were passed over a chitin resin to remove the Intein-containing proteins (lane 6). The MBP was removed using a phosphocellulose resin to generate homogeneous TREX2 (lane 7). Samples were subjected to 12% SDS-PAGE, and the gel was stained with Coomassie Brilliant Blue. The positions of migration of the MBP-Intein-TREX2 (MYCT2), *Sce* VMA intein(CBD), MBP, TREX2, and molecular weight standards (lane 1) are indicated.

C-termini of the Intein. The His to Gln substitution at the penultimate amino acid of the Intein prevents the splicing reaction characteristic of the wild-type *Sce* VMA intein (Chong et al., 1998). Further, it was necessary to modify the TREX2 gene to prevent in vivo cleavage of the Intein construct by including two additional amino acids (Ala–Gly) that are retained at the N-terminus of TREX2 upon Intein cleavage. The self-cleaving activity of the Intein in this construct is exhibited upon addition of dithiothreitol and results in the production of the three proteins MBP, Intein(CBD), and TREX2 after completion of the Intein cleavage reaction (Fig. 3, lane 5). The Intein protein contains a chitin binding domain and is removed from the preparation along with any uncleaved fusion protein by passing the sample over a chitin resin (Fig. 3, lane 6). The TREX2 protein binds tightly to a phosphocellulose resin and is easily separated from the MBP that flows through the column (Fig. 3, lane 7). This expression strategy results in the production of about 4–8 mg of homogeneous TREX2 protein per liter of starting bacterial culture providing abundant quantities of the TREX2 enzyme for structural and mechanistic studies.

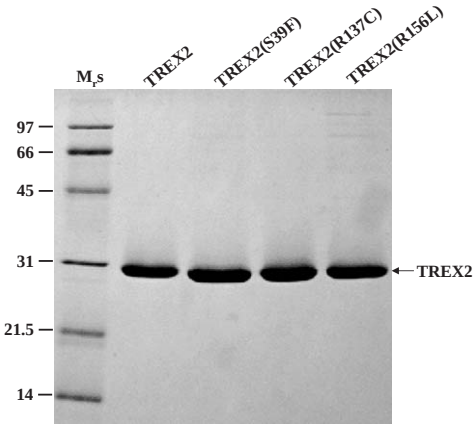

Fig. 4. SDS-PAGE analysis of the purified TREX2 and TREX2 variant proteins. Site-directed mutations were introduced into the MBP-Intein-TREX2 plasmid to generate the TREX2 SNP variant genes. The TREX2(S39F), TREX2(R137C), and TREX2(R156L) proteins were generated as described in the text for TREX2. Approximately 3 μg of each protein was subjected to 12% SDS-PAGE, and the gel was stained with Coomassie Brilliant Blue. The positions of migration of the TREX2 proteins and the molecular weight standards (lane 1) are indicated.

The three TREX2 variant proteins identified in the genetic screen were also produced using this bacterial expression system in order to investigate possible alterations in the catalytic properties of the variant TREX2 $3' \rightarrow 5'$ deoxyribonucleases. Similar results were obtained in the purification of the TREX2 variant proteins. An SDS-PAGE analysis of 3 μg of each TREX2 protein is shown in Fig. 4. The staining intensities indicate the similar quantities of proteins.

Excision activities of TREX2 and the TREX2-S39F, -R137C, and -R156L proteins

The TREX2 and variant proteins were examined for $3' \rightarrow 5'$ deoxyribonuclease activity using a dT_{20} oligonucleotide to confirm the presence of this activity in each of the TREX2 proteins and to establish the relative 3′ nucleotide excision activities for the variant TREX2 proteins (Fig. 5). Incubation of increased amounts of TREX2 (Fig. 5, lanes 1–5), TREX2-S39F (Fig. 5, lanes 6–10), TREX2-R137C (Fig. 5, lanes 11–15), and TREX2-R156L (Fig. 5, lanes 16–20) resulted in increased degradation of the dT_{20} substrate similarly establishing the presence of the robust catalytic activity in the TREX2 variants that is characteristic of the wild-type TREX2 protein (Mazur and Perrino, 2001a). The rates of 3′ nucleotide excision were determined by quantifying the 3′ dTMP excised from the dT_{20} substrate in the presence of three different enzyme concentrations (Table 1). Reaction rates determined in the presence of these enzyme amounts are in the linear range of the assay for all of the TREX2 proteins. These results indicate similar catalytic rates for the TREX2 variant proteins relative to the wild-type TREX2.

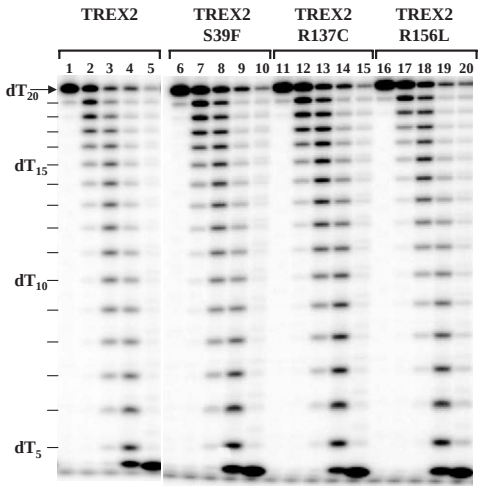

Fig. 5. The $3' \rightarrow 5'$ deoxyribonuclease activities of TREX2 and the TREX2 variant proteins. Standard exonuclease reactions (10 μl) were prepared with a ^{32}P-labeled dT_{20} oligonucleotide and dilutions of the TREX2 enzymes were prepared at 10 times the final concentrations. Samples (1 μl) containing 5 pg (lanes 2, 7, 12, and 17), 20 pg (lanes 3, 8, 13, and 18), 80 pg (lanes 4, 9, 14, and 18), or 320 pg (lanes 5, 10, 15, and 20) of the indicated TREX2 enzymes were added to reactions. Incubations were 20 min at 25°C. Reaction products were subjected to electrophoresis on 23% polyacrylamide gels. The positions of migration of the dT_{20} and products are indicated.

Steady-state kinetics of the TREX2 proteins

To more precisely quantify the $3' \rightarrow 5'$ deoxyribonuclease activities of the TREX2 variant proteins the apparent rate constants (K_M and k_{cat}) for excision of dTMP from a dT_{20} oligomer were determined. Excision by TREX2 and the variant proteins was measured in the presence of increased concentrations of the dT_{20} oligomer ranging from 5 to 500 nM (Fig. 6). The K_M and k_{cat} values determined for the TREX2 proteins are summarized in Table 2. Like the activity measurements shown in Table 1 there are only modest differences in the measured K_M and k_{cat} values and the second-order rate constants (k_{cat}/K_M) calculated for these variant TREX2 proteins (Table 2). The 50% higher activity determined for the TREX2-S39F relative to TREX2 (Table 1) is also apparent in the two-fold higher calculated efficiency (k_{cat}/K_M) (Table 2). The k_{cat} value for TREX2-S39F is nearly three-fold higher than that of TREX2. Likewise, the nearly two-fold lower activity of the TREX2-R156L relative to TREX2 (Table 1) is similar to the lower catalytic efficiency measured for the TREX2-R156L enzyme (Table 2). These apparent differences in the kinetic constants for the TREX2 variant proteins are not likely explained by differences in the initial quantification of the proteins as similar staining intensities are observed upon electrophoresis of 3 μg of each protein in a SDS-PAGE analysis (Fig. 4). However, these enzymatic assays require 50,000-fold dilutions of the enzymes making it difficult to eliminate small variations that might occur during this dilution process. Thus, it seems most likely that the TREX2 variant proteins are sequence

Table 1
Catalytic activities of TREX2 and the TREX2 variant proteins

Enzyme	Amount[a] (pg)	Activity[b] (fmol/s/fmolE)	Average activity[c] (fmol/s/fmolE)	Relative activity[d]
TREX2	1	4.3		
	5	2.9	3.1 ± 0.19	1.0
	20	3.1		
TREX2-S39F	1	8.8		
	5	5.0	4.8 ± 0.098	1.5
	20	4.9		
TREX2-R137C	1	3.2		
	5	3.2	2.8 ± 0.25	0.90
	20	2.8		
TREX2-R156L	1	1.8		
	5	1.5	1.8 ± 0.11	0.58
	20	1.8		

[a] Reactions (10 μl) were prepared using 1, 5, or 20 pg (in triplicate) of the TREX2 proteins (1 pg = 0.038 fmol) in standard exonuclease reactions. Incubations were 20 min at 25°C.

[b] Products were separated on polyacrylamide gels, and activity was quantified as described under "Materials and methods."

[c] Plots of activity vs. enzyme concentrations were generated using the three different enzyme concentrations in triplicate reactions to confirm linearity of the assay and to generate the average activity values.

[d] Relative activity is in $(\text{fmol/s/fmol}_{\text{SNP}})/(\text{fmol/s/fmol}_{\text{TREX2}})$.

variations of the TREX2 gene that encode proteins with fully functional $3' \rightarrow 5'$ deoxyribonucleases. While the catalytic functions of these variant TREX2 proteins appear unaffected by these SNPs it is possible that these enzymes are altered in some capacity that is not revealed by measuring the 3′ excision activity using this short single stranded dT_{20} substrate.

Summary

A genetic analysis of the TREX2 gene identified eleven SNPs: three of these SNPs were missense polymorphisms resulting in the TREX2-S39F, -R137C, and -R156L proteins. A novel bacterial expression system was used to generate these TREX2 proteins for biochemical analysis. Quantification of the activities and kinetic constants of the variant proteins demonstrate that all of these enzymes exhibit robust $3' \rightarrow 5'$ deoxyribonuclease activities comparable to TREX2. These results are consistent with the recently determined X-ray structure of the native TREX2 protein (T. Hollis, unpublished results) which indicates that the amino-acid substitutions in the TREX2 variants are positioned in regions of the protein not likely to directly impact on catalytic function. The 3′ nucleotide excision properties

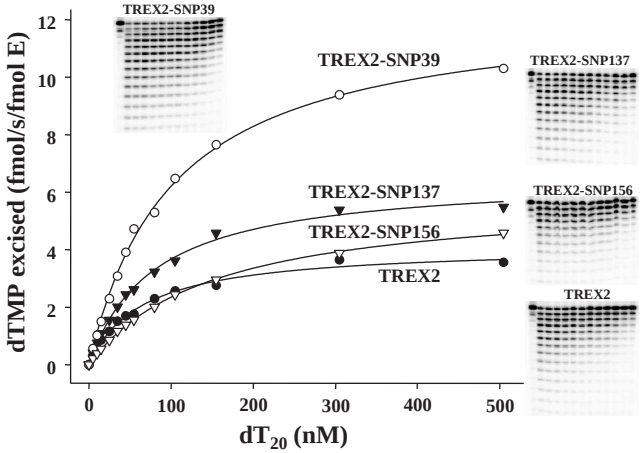

Fig. 6. Steady-state kinetic analysis of the 3′→5’ deoxyribonuclease activities of TREX2 and the TREX2 variant proteins. Standard exonuclease reactions (10 μl) were prepared containing the TREX2 enzymes (10 pg), the ^{32}P-labeled dT_{20} oligonucleotide (5 nM), and additions of unlabeled dT_{20} oligonucleotide ranging from 0 to 500 nM. Incubations were 20 min at 25°C. Reaction products were subjected to electrophoresis on 23% polyacrylamide gels (see insets). The products were quantified, and the kinetic constants (Table 2) were determined as described under ‘‘Materials and methods.’’

Table 2
Steady-state kinetics of the TREX2 and variant proteins

Enzyme	K_M[a]	k_{cat}	k_{cat}/K_M	Relative efficiency[b]
	M($x10^{-9}$)	s^{-1}	M^{-1} s^{-1}	
TREX2	65±4.8	4.1±0.11	6.3×10^7	1.0
TREX2-S39F	100±4.2	12±0.21	1.2×10^8	1.9
TREX2-R137C	79±4.4	6.6±0.14	8.4×10^7	1.3
TREX2-R156L	150±3.8	5.9±0.067	3.9×10^7	0.62

[a] Reactions (10 μl) were prepared using 10 pg of the TREX2 proteins (1 pg = 0.038 fmol) and dT_{20} at concentrations ranging from 5 to 500 nM. Incubations were 20 min at 25°C. Products were separated on polyacrylamide gels (Fig. 6) and quantified as described under ‘‘Materials and methods.’’

[b] Relative efficiency is in $(M^{-1} s^{-1}_{SNP})/(M^{-1} s^{-1}_{TREX2})$.

of these TREX2 enzymes support the idea that the proteins encoded by the TREX2 SNPs are fully functional 3′→5′ deoxyribonucleases. However, it is possible that diminished cellular function of these TREX2 SNPs is facilitated through alterations it partnering proteins during the processes of DNA replication, repair, or recombination.

References

Bessho T, Sancar A. Human DNA damage checkpoint protein hRAD9 is a 3′ to 5′ exonuclease. J Biol Chem 2000;275:7451–4.

Bialek G, Grosse F. An error-correcting proofreading exonuclease-polymerase that copurifies with DNA-polymerase-α-primase. J Biol Chem 1993;268:6024–33.

Brown KR, Weatherdon KL, Galligan CL, Skalski V. A nuclear 3′–5′ exonuclease proofreads for the exonuclease-deficient DNA polymerase alpha. DNA Repair 2002;1:795–810.

Burgers PMJ, Koonin EV, Bruford E, Blanco L, Burtis KC, Christman MF, Copeland WC, Friedberg EC, Hanaoka F, Hinkle DC, Lawrence CW, Nakanishi M, Ohmori H, Prakash L, Prakash S, Reynaud CA, Sugino A, Todo T, Wang ZG, Weill JC, Woodgate R. Eukaryotic DNA polymerases: proposal for a revised nomenclature. J Biol Chem 2001;276:43487–90.

Chaudhry MA, Dedon PC, Wilson 3rd DM, Demple B, Weinfeld M. Removal by human apurinic/apyrimidinic endonuclease 1 (Ape 1) and *Escherichia coli* exonuclease III of 3′-phosphoglycolates from DNA treated with neocarzinostatin, calicheamicin, and gamma-radiation. Biochem Pharmacol 1999;57:531–8.

Chong SR, Williams KS, Wotkowicz C, Xu MQ. Modulation of protein splicing of the *Saccharomyces cerevisiae* vacuolar membrane ATPase intein. J Biol Chem 1998;273:10567–77.

Chou KM, Kukhanova M, Cheng YC. A novel action of human apurinic/apyrimidinic endonuclease: excision of L-configuration deoxyribonucleoside analogs from the 3′ termini of DNA. J Biol Chem 2000;275:31009–15.

Gill SC, von Hippel PH. Calculation of protein extinction coefficients from amino acid sequence data [published erratum appears in Anal Biochem 1990 189; 283]. Anal Biochem 1989;182:319–26.

Higuchi R. A guide to methods and applications. In: Innis MA, Gelfand DH, Sninsky JJ, White TJ (editors). PCR protocols. San Diego, CA: Academic Press; 1990. p. 177–83.

Hollis GF, Grossman L. Purification and characterization of DNase VII, a 3′→5′-directed exonuclease from human placenta. J Biol Chem 1981;256:8074–9.

Hoss M, Robins P, Naven TJ, Pappin DJ, Sgouros J, Lindahl T. A human DNA editing enzyme homologous to the *Escherichia coli* DnaQ/MutD protein. EMBO J 1999;18:3868–75.

Huang S, Li B, Gray MD, Oshima J, Mian IS, Campisi J. The premature ageing syndrome protein, WRN, is a 3′→5′ exonuclease. Nat Genet 1998;20:114–6.

Kamath-Loeb AS, Shen JC, Loeb LA, Fry M. Werner syndrome protein—II: characterization of the integral 3′→5′-DNA exonuclease. J Biol Chem 1998;273:34145–50.

Lindahl T, Gally JA, Edelman GM. Properties of deoxyribonuclease III from mammalian tissues. J Biol Chem 1969;244:5014–9.

Mazur DJ, Perrino FW. Excision of 3′ termini by the Trex1 and TREX2 3′→5′ exonucleases: characterization of the recombinant proteins. J Biol Chem 2001a;276:17022–9.

Mazur DJ, Perrino FW. Identification and expression of the TREX1 and TREX2 cDNA sequences encoding mammalian 3′→5′ exonucleases. J Biol Chem 1999;274:19655–60.

Mazur DJ, Perrino FW. Structure and expression of the TREX1 and TREX2 3′→5′ exonuclease genes. J Biol Chem 2001b;276:14718–27.

Modrich P. Strand-specific mismatch repair in mammalian cells. J Biol Chem 1997;272:24727–30.

Mosbaugh DW, Meyer RR. Interaction of mammalian deoxyribonuclease V, a double strand 3′→5′ and 5′→3′ exonuclease with deoxyribonucleic acid polymerase β from the Novikoff hepatoma. J Biol Chem 1980;255:10239–47.

Mummenbrauer T, Janus F, Müller B, Wiesmüller L, Deppert W, Grosse F. p53 protein exhibits 3′-to-5′ exonuclease activity. Cell 1996;85:1089–99.

Parker AE, Van de Weyer I, Laus MC, Oostveen I, Yon J, Verhasselt P, Luyten WH. A human homologue of the *Schizosaccharomyces pombe* rad1+ checkpoint gene encodes an exonuclease. J Biol Chem 1998;273:18332–9.

Paull TT, Gellert M. The 3′ to 5′ exonuclease activity of Mre 11 facilitates repair of DNA double-strand breaks. Mol Cell 1998;1:969–79.

Paull TT, Gellert M. A mechanistic basis for Mre11-directed DNA joining at microhomologies. Proc Natl Acad Sci 2000;97:6409–14.

Perrino FW, Mazur DJ, Ward H, Harvey S. Exonucleases and the incorporation of aranucleotides into DNA. Cell Biochem Biophys 1999;30:331–52.

Perrino FW, Miller H, Ealey KA. Identification of a 3′→5′-exonuclease that removes cytosine arabinoside monophosphate from 3′ termini of DNA. J Biol Chem 1994;269:16357–63.

Shen JC, Gray MD, Oshima J, Ashwini SK, Fry M, Loeb LA. Werner syndrome protein I: DNA helicase and DNA exonuclease reside on the same polypeptide. J Biol Chem 1998;273:34139–44.

Skalski V, Liu SH, Cheng YC. Removal of anti-human immunodeficiency virus 2′,3′-dideoxynucleoside monophosphates from DNA by a novel human cytosolic 3′→5′ exonuclease. Biochem Pharmacol 1995;50:815–21.

Skarnes W, Bonin P, Baril E. Exonuclease activity associated with a multiprotein form of HeLa cell DNA polymerase α. J Biol Chem 1986;261:6629–36.

Smith JR, Freije D, Carpten JD, Gronberg H, Xu JF, Isaacs SD, Brownstein MJ, Bova GS, Guo H, Bujnovszky P, Nusskern DR, Damber JE, Bergh A, Emanuelsson M, Kallioniemi OP, WalkerDaniels J, BaileyWilson JE, Beaty TH, Meyers DA, Walsh PC, Collins FS, Trent JM, Isaacs WB. Major susceptibility locus for prostate cancer on chromosome 1 suggested by a genome-wide search. Science 1996;274:1371–4.

Thelen MP, Onel K, Holloman WK. The REC1 gene of *Ustilago maydis* involved in the cellular response to DNA damage encodes an exonuclease. J Biol Chem 1994;269:747–54.

Wilson 3rd DM, Takeshita M, Grollman AP, Demple B. Incision activity of human apurinic endonuclease (Ape) at abasic site analogs in DNA. J Biol Chem 1995;270:16002–7.

Xu JF, Meyers D, Freije D, Isaacs S, Wiley K, Nusskern D, Ewing C, Wilkens E, Bujnovszky P, Bova GS, Walsh P, Isaacs W, Schleutker J, Matikainen M, Tammela T, Visakorpi T, Kallioniemi OP, Berry R, Schaid D, French A, McDonnell S, Schroeder J, Blute M, Thibodeau S, Gronberg H, Emanuelsson M, Damber JE, Bergh A, Jonsson BA, Smith J, Bailey-Wilson J, Carpten J, Stephan D, Gillanders E, Amundson I, Kainu T, Freas-Lutz D, Baffoe-Bonnie A, Van Aucken A, Sood R, Collins F, Brownstein M, Trent J. Evidence for a prostate cancer susceptibility locus on the X chromosome. Nat Genet 1998;20:175–9.